Statistical modeling of competitive threshold collision-induced dissociation

M. T. Rodgers
Department of Chemistry, Wayne State University, Detroit, Michigan 48202

P. B. Armentrout
Department of Chemistry, University of Utah, Salt Lake City, Utah 84112

(Received 30 March 1998; accepted 27 April 1998)

Collision-induced dissociation of $(R_1OH)Li^+(R_2OH)$ with xenon is studied using guided ion beam mass spectrometry. R_1OH and R_2OH include the following molecules: water, methanol, ethanol, 1-propanol, 2-propanol, and 1-butanol. In all cases, the primary products formed correspond to endothermic loss of one of the neutral alcohols, with minor products that include those formed by ligand exchange and loss of both ligands. The cross-section thresholds are interpreted to yield 0 and 298 K bond energies for $(R_1OH)Li^+$–R_2OH and relative Li^+ binding affinities of the R_1OH and R_2OH ligands after accounting for the effects of multiple ion–molecule collisions, internal energy of the reactant ions, and dissociation lifetimes. We introduce a means to simultaneously analyze the cross sections for these competitive dissociations using statistical theories to predict the energy dependent branching ratio. Thermochemistry in good agreement with previous work is obtained in all cases. In essence, this statistical approach provides a detailed means of correcting for the ''competitive shift'' inherent in multichannel processes. © *1998 American Institute of Physics.* [S0021-9606(98)02729-9]

INTRODUCTION

In recent work,[1] we measured the binding energies of Li^+ to multiple H_2O ligands, including the first direct measurement of the $Li^+(H_2O)$ bond energy, using collision-induced dissociation (CID) methods. These values were compared to the results of Dzidic and Kebarle (DK)[2] who used high pressure mass spectrometry (HPMS). Good agreement was obtained for $Li^+(H_2O)_n$, $n=2-5$; however, the value we obtained for $Li^+(H_2O)_6$ was higher than that measured by DK. In the case of $Li^+(H_2O)$, our directly measured value was somewhat lower than the value given by DK, which was not measured directly, but extrapolated from their values for larger $Li^+(H_2O)_n$ clusters. Because the Li^+ binding affinity scale has been anchored using DK's value for $Li^+(H_2O)$, it would be useful to establish its absolute bond energy with high accuracy. Although direct CID studies of this complex provide a reasonable bond energy, the experiment was not as straightforward to perform and interpret as is common in our laboratory. Hence, we sought an alternative method to independently determine the $Li^+(H_2O)$ bond energy.

In other recent experiments,[3] we have measured the Li^+ binding affinities to short chain alcohols. The binding energies of Li^+ to water and the alcohols have been studied by equilibrium methods in an ion cyclotron resonance (ICR) mass spectrometer by Beauchamp and co-workers[4,5] and by Taft *et al.*[6] The absolute Li^+ affinities reported by Woodin and Beauchamp (as well as other studies throughout the literature) can be traced back to the extrapolated value of $D(Li^+–OH_2)$ reported by DK.[2] Good agreement for the binding energy of $Li^+(CH_3OH)$ was obtained between our work and that of Beauchamp and co-workers. The relative affinities of the alcohols measured by Taft *et al.*[6] also agreed nicely with our work; however, Taft's absolute values were said to be referenced to values determined by Woodin and Beauchamp,[5] but improperly corrected for differing experimental temperatures as discussed in detail elsewhere.[3]

After completing these studies, it occurred to us that an accurate value for the $Li^+(H_2O)$ bond energy could be determined by measuring its Li^+ affinity relative to one or more of the alcohols. This can be achieved by examining the CID of $(H_2O)Li^+(ROH)$ complexes. To verify that reasonable numbers can be provided in this fashion, we have also examined a number of $(R_1OH)Li^+(R_2OH)$ complexes incorporating two different alcohols. In the present study, we use guided ion beam mass spectrometry to collisionally excite these simple complexes: Li^+ bound to water and simple alcohols, $(R_1OH)Li^+(R_2OH)$, where R_1OH and R_2OH=water, methanol (MeOH), ethanol (EtOH), 1-propanol (1-PrOH), 2-propanol (2-PrOH), and 1-butanol (1-BuOH). Strong competitive dissociation of both ligands is observed. We demonstrate that the analysis of these strongly competitive dissociations cannot be accurately performed without explicitly considering the effect of the competition on the shapes of the cross sections. In this work, we develop a statistical procedure that extends the methods that we have previously developed for the analysis of CID threshold behavior to such competitive processes. This is shown to provide an accurate means of analyzing the data and provides substantial support for our assumption of a very loose transition state for CID processes involving electrostatically bound species.[7] This statistical approach provides a straightforward, albeit somewhat computationally intensive, procedure for correcting for the ''competitive shift'' inherent in multi-channel processes.

EXPERIMENT

General procedures

Cross sections for CID of $(R_1OH)Li^+(R_2OH)$, where R_1OH and R_2OH are water, methanol, ethanol, 1-propanol, 2-propanol, or 1-butanol, are measured using a guided ion beam mass spectrometer that has been described in detail previously.[8,9] The dimer complexes are generated as described below. The ions are extracted from the source, accelerated, and focused into a magnetic sector momentum analyzer for mass analysis. Mass-selected ions are decelerated to a desired kinetic energy and focused into an octopole ion guide which traps the ions in the radial direction.[10] The octopole passes through a static gas cell containing xenon, used as the collision gas, for reasons described elsewhere.[11–13] Low gas pressures in the cell (typically 0.04 to 0.20 mTorr) are used to ensure that multiple ion–molecule collisions are improbable. Product and unreacted beam ions drift to the end of the octopole where they are focused into a quadrupole mass filter for mass analysis and subsequently detected with a secondary electron scintillation detector and standard pulse counting techniques.

Ion intensities are converted to absolute cross sections as described previously.[8] Absolute uncertainties in cross section magnitudes are estimated to be $\pm 20\%$ which is largely the result of error in the pressure measurement and the length of the interaction region. Relative uncertainties are approximately $\pm 5\%$. Because the radio frequency used for the octopole does not trap light masses with high efficiency, the cross sections for Li^+ products were more scattered and showed more variations in magnitude than is typical for this apparatus. Therefore, absolute magnitudes of the cross sections for production of Li^+ are probably $\pm 50\%$.

Ion kinetic energies in the laboratory frame, E_{Lab}, are converted to energies in the center of mass frame, E_{CM}, using the formula $E_{CM}=E_{lab}m/(m+M)$, where M and m are the masses of the ionic and neutral reactants, respectively. All energies reported below are in the CM frame unless otherwise noted. The absolute zero and distribution of the ion kinetic energies are determined using the octopole ion guide as a retarding potential analyzer as previously described.[8] The distribution of ion kinetic energies is nearly Gaussian with a FWHM typically between 0.2 and 0.3 eV (Lab) for these experiments. The uncertainty in the absolute energy scale is ± 0.05 eV (Lab).

Even when the pressure of the reactant neutral is low, we have previously demonstrated that the effects of multiple collisions can significantly influence the shape of CID cross sections.[14] Because the presence and magnitude of these pressure effects is difficult to predict, we have performed pressure dependent studies of all cross sections examined here. In the present systems, we observe small cross sections at low energies that have an obvious dependence upon pressure. We attribute this to multiple energizing collisions that lead to an enhanced probability of dissociation below threshold as a result of the longer residence time of these slower moving ions. Data free from pressure effects is obtained by extrapolating to zero reactant pressure, as described previously.[14] Thus results reported below are due to single bimolecular encounters.

Ion source

The $(R_1OH)Li^+(R_2OH)$ complexes are formed in a 1 m long flow tube[9,15] operating at a pressure of 0.5–0.7 Torr with a helium flow rate of 4000–7000 sccm. Metal ions are generated in a continuous dc discharge by argon ion sputtering of a cathode, made from tantalum or iron, with a cavity containing lithium metal. Typical operating conditions of the discharge are 2–3 kV and 20–30 mA in a flow of roughly 10% argon in helium. The $(R_1OH)Li^+(R_2OH)$ complexes are formed by associative reactions of the lithium ion with water and the neutral alcohols which are introduced into the flow 50 cm downstream from the dc discharge. The flow conditions used in this ion source provide in excess of 10^4 collisions between an ion and the buffer gas, which should thermalize the ions both vibrationally and rotationally. In our analysis of the data, we assume that the ions produced in this source are in their ground electronic states and that the internal energy of the $(R_1OH)Li^+(R_2OH)$ complexes is well described by a Maxwell–Boltzmann distribution of rovibrational states at 300 K. Previous work from this laboratory has shown that these assumptions are generally valid.[11,14–19]

DATA ANALYSIS

Background

Our analysis of the energy dependence of CID cross sections utilizes Eq. (1)

$$\sigma(E)=\sigma_0\sum_i g_i(E+E_i-E_0)^n/E, \tag{1}$$

where E is the relative collision energy, E_0 is the reaction threshold at 0 K, σ_0 is an energy independent scaling factor, and n is an adjustable parameter. The summation is over the rovibrational states of the reactants having energies E_i and populations g_i, where $\Sigma g_i=1$. The relative reactivities of all rovibrational states, as reflected by σ_0 and n, are assumed to be equivalent. The Beyer–Swinehart algorithm[20] is used to evaluate the density of the rovibrational states and the relative populations g_i are calculated by an appropriate Maxwell–Boltzmann distribution at the temperature appropriate for the reactants.

To incorporate unimolecular dissociation theory into Eq. (1), we integrate over a dissociation probability determined from the set of rovibrational frequencies appropriate for the energized molecule (EM) and the transition state (TS) leading to dissociation. As described in detail elsewhere,[7,16] the expression for the total cross section is

$$\sigma_{tot}(E)=(n\sigma_0/E)\sum_i g_i\int_0^{E+E_i-E_0}[1-e^{-k_{tot}(E+E_i-\Delta E)\tau}]\times(\Delta E)^{n-1}d(\Delta E), \tag{2}$$

where most parameters are the same as in Eq. (1), τ is the experimental time available for dissociation, and $k_{tot}(E+E_i-\Delta E)$ is the total unimolecular rate constant. The term ΔE is the energy that remains in translation after the collision be-

tween the reactants, hence $E-\Delta E$ is the energy transferred to the internal modes of the dissociating ion by this collision at a relative translational energy E. Thus the internal energy of EM after the collision is $E^*=E+E_i-\Delta E$. The unimolecular rate constant $k_{tot}(E^*)$ is defined in the usual manner by RRKM theory,[21–23]

$$k_{tot}(E^*)=\sum_j k_j(E^*)=\sum_j d_j N_j^{\dagger}(E^*-E_{0,j})/h\rho(E^*), \tag{3}$$

where $k_j(E^*)$ is the rate constant for a single dissociation channel j, d_j is the reaction degeneracy for channel j ($d_j=l_j^{\ddagger}\sigma_r/\sigma_{rj}^{\dagger}$, where $l_j^{\ddagger}$ is the number of optical isomers of the TS and $\sigma_r/\sigma_{rj}^{\dagger}$ is the ratio of rotational symmetry numbers of the EM and TS for channel j),[21,23] $N_j^{\dagger}(E^*-E_{0,j})$ is the sum of rovibrational states of the TS for channel j at an energy $E^*-E_{0,j}$, $E_{0,j}$ is the dissociation energy for channel j, and $\rho(E^*)$ is the density of states of the EM at the energy available, E^*. Equation (2) was designed so that it reduces to Eq. (1) in the limit that the total unimolecular decay rate is fast for all values of ΔE in the integral [hence, the term in Eq. (2) in square brackets reduces to unity]. The summation over the various dissociation channels j is introduced into this treatment for the first time here, otherwise the formulas are the same as previously used for analyses of kinetic energy dependent CID where dissociation is dominated by a single channel.[7,16]

To describe the cross section for an individual reaction channel, σ_j, we refer to the kinetic solution for a unimolecular dissociation process, $A^*\xrightarrow{k_j}P_j$, namely $[A^*]=[A^*]_0\exp(-k_{tot}\tau)$ and $[P_j]=(k_j/k_{tot})[A^*]_0[1-\exp(-k_{tot}\tau)]$, where $\Sigma k_j=k_{tot}$. Given these relationships, it is tempting to simply assign $\sigma_j=(k_j/k_{tot})\sigma_{tot}$, but this fails to properly account for the distribution in excitation energy E^* which influences the competition. Instead, we modify Eq. (2) to yield Eq. (4)

$$\sigma_j(E)=(n\sigma_{0,j}/E)\sum_i g_i\int_0^{E+E_i-E_0}[k_j(E^*)/k_{tot}(E^*)]\times[1-e^{-k_{tot}(E^*)\tau}](\Delta E)^{n-1}d(\Delta E). \tag{4}$$

This shows that the cross sections for individual dissociation channels are indeed coupled through the k_{tot} terms. It is worth noting that the ratio of k_j to k_{tot} can be simplified to Eq. (5)

$$k_j(E^*)/k_{tot}(E^*)=d_jN_j^{\dagger}(E^*-E_{0,j})\Big/\sum_j d_jN_j^{\dagger}(E^*-E_{0,j}). \tag{5}$$

Ideally, values for $\sigma_{0,j}$, the energy independent scaling factors for each channel, should be equal; however, empirically, we find that this constraint does not allow some of the data to be reproduced with high accuracy. This is discussed further below.

Thermochemical analysis

The threshold regions of the reaction cross sections are modeled using Eqs. (2) and (4). To evaluate the energies of the rovibrational states needed in these equations, semi-

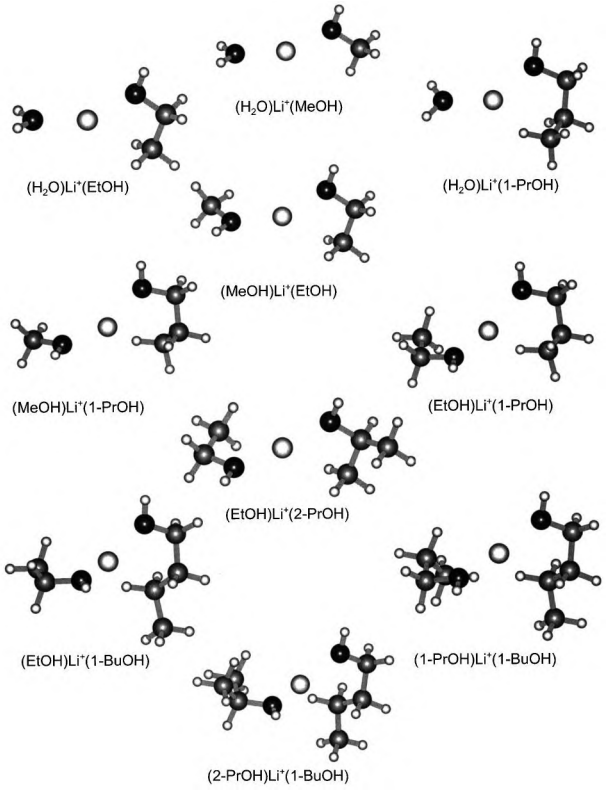

FIG. 1. Semiempirical PM3-optimized geometries of $(R_1OH)Li^+(R_2OH)$ complexes where R_1OH and R_2OH=water, methanol, ethanol, 1-propanol, 2-propanol, and 1-butanol.

empirical calculations were performed with HYPERCHEM[24] for the neutral alcohols, lithiated alcohols, and mixed lithium bound alcohol dimers. Calculations were performed using the PM3[25–27] method. In all of the calculations, starting structures are annealed and then energy minimized. The geometry optimized structures of the lithium bound alcohol dimers determined at the semiempirical PM3 level are shown in Fig. 1. In all cases, the lithium ion prefers to be bound to the oxygen atoms. The hydrocarbon backbone wraps around the lithium ion in such a way as to maximize the electrostatic interaction between the lithium ion and the alcohol while minimizing steric repulsion between the two alcohols. The Li^+ affinities calculated at this level of theory are significantly lower than the experimentally determined values. This appears to be largely because Li^+ retains about 0.8–0.9 of its charge in its adducts,[28] whereas the PM3 calculations indicate that only 0.7–0.8 of the positive charge is retained by Li^+. The decreased charge retention by Li^+ in the calculated structures leads to longer Li^+–O bond distances, which ranged from 2.07–2.12 Å in the $Li^+(ROH)$ complexes. For $Li^+(H_2O)$, PM3 calculations performed here yield a Li^+–O bond distance of 2.05 Å, while more sophisticated calculations give 1.85 Å.[29] Potentially, such discrepancies could influence the rotational constants used to model the data, however, the means used to estimate the uncertainties that result from these rotational constants (see below) already incorporate this 10% error in bond length.

A vibrational analysis of the geometry optimized structures is performed to determine the vibrational frequencies

and rotational constants of the molecules. We have scaled the vibrational frequencies obtained in our analyses by a factor of 0.9 as suggested by recent work.[30,31] The scaled vibrational frequencies thus obtained using the PM3 method for the $(R_1OH)Li^+(R_2OH)$ complexes are listed in Table I (supplementary material).[32] Those for the neutral ligands and the monoligated complexes can be found in Refs. 1 and 3. It was found that the lowest frequency calculated for the mixed dimers was not reliable (negative in some cases and exceedingly low in others). This mode corresponds to the torsional motion where the two ligands rotate about the O–Li–O bond axis in opposite directions. Thus this motion is more appropriately described and was therefore treated as a one dimensional rotor, for which the rotational constant was evaluated as outlined by Gilbert and Smith.[21] Rotational constants of all species (including the torsions of the mixed dimers) are listed in Table II (supplementary material).[32] The Beyer–Swinehart algorithm[20,21] is used to calculate the population distribution of rovibrational states using these frequencies and rotational constants.

The average vibrational energy at 298 K of the lithium bound alcohol dimers is also given in Table I.[32] References 1 and 3 provide this information for the neutral and lithiated alcohols. We have estimated the sensitivity of our analysis to the deviations from the true frequencies by scaling the originally calculated PM3 frequencies to encompass the range of average valence coordinate scale factors needed to bring calculated frequencies into agreement with experimentally determined frequencies found by Seeger *et al.*[30] All of the originally calculated vibrational frequencies were scaled by 0.7 and 1.1. The corresponding change in the average vibrational energy is taken to be an estimate of one standard deviation of the uncertainty in vibrational energy and is included in the uncertainties listed with the E_0 and $E_{0,j}$ values. This variation in frequencies is also the overwhelming source of the reported uncertainties in the entropies of activation determined for each dissociation reaction (see below). We believe this variation is a very conservative estimate of the errors in these frequencies and the resultant thresholds and entropies of activation.

Equations (2) and (4) explicitly consider whether dissociation occurs within the time scale of the experiment, approximately 10^{-4} s in our instrument. If the lifetime of the collisionally excited ion exceeds this, then a kinetic shift will be observed as an increase in the apparent threshold to higher kinetic energies. To evaluate the rate constants in Eqs. (2) and (4), sets of rovibrational frequencies appropriate for the energized molecule and the transition states leading to dissociation are required. These are derived from the frequencies and rotational constants listed in Tables I and II[32] and Refs. 1 and 3. Choices for the molecular parameters of the TS can be estimated with two limiting assumptions and a choice that reflects the most probable TS. In the first limit, lifetime effects are ignored (in essence, this assumes that the rate of dissociation at all collision energies is faster than the experimental time scale). At the other extreme, an upper limit to the kinetic shift is provided by a tight TS, where the molecular parameters of the TS are assumed to equal those of the dissociating molecule minus the single mode that corresponds to the reaction coordinate. The reaction coordinate (identified by boldface type in Table I[32]) is associated with the O–Li–O asymmetric stretch. Because the interaction between the lithium ion and the ligands is largely electrostatic, the most appropriate model for estimating the lifetime effect should be a loose TS. In this case, the TS vibrations used are the frequencies corresponding to the products and are found in Refs. 1 and 3. The transitional frequencies, those that become rotations of the completely dissociated products, are treated as rotors, a treatment that corresponds to a phase space limit (PSL) and is described in detail elsewhere.[7] For the $(R_1OH)Li^+(R_2OH)$ complexes, the five transitional mode rotors have rotational constants equal to those of the $Li^+(R_1OH)$ and R_2OH products with axes perpendicular to the reaction coordinate. These are listed in Table II.[32] The external rotations of the energized molecule and TS are also included in the modeling of the CID data. The external rotational constants of the TS are determined by assuming that the TS state occurs at the centrifugal barrier for interaction of $(R_1OH)Li^+$ with R_2OH, calculated variationally as outlined elsewhere.[7] The 2-D external rotations are treated adiabatically but with centrifugal effects included consistent with the discussion of Waage and Rabinovitch.[33] Because the distribution of rotational energies of the EM created in a collisional process is not well characterized, we have outlined several reasonable assumptions appropriate for collisional activation elsewhere.[7] In the present work, we tested both the equipartitioning and statistical assumptions in which the average 2-D external rotational energy is used. These two assumptions yield comparable results except when one of the ligands is water. In this case, it was found that the statistical assumption (which we believe is the most appropriate) provides much better agreement with literature thermochemistry than the equipartitioning assumption. Evidently, this is because equipartitioning places too much energy in the 2-D rotations for a molecule like water which has relatively large rotational constants. Based on this observation, the results reported below utilize the statistical assumption in all cases.

The model represented by Eqs. (1), (2), and (4) is expected to be appropriate for translationally driven reactions.[34] This model form has been found to reproduce reaction cross sections well in a number of previous studies of both atom–diatom and polyatomic reactions,[35,36] including CID processes.[1,3,11,14–16,37,38] It is assumed that n and σ_0 or $\sigma_{0,j}$ in Eqs. (2) and (4) are the same for all states. The model is convoluted with the kinetic energy distribution of the reactants, and a nonlinear least-squares analysis of the data is performed to give optimized values for the parameters σ_0 or $\sigma_{0,j}$, E_0 or $E_{0,j}$, and n. The error associated with the measurement of E_0 or $E_{0,j}$ is estimated from the range of threshold values determined for different data sets, variations associated with uncertainties in the vibrational frequencies, and the error in the absolute energy scale, 0.05 eV (Lab). For analyses that include the RRKM lifetime effect, the uncertainties in the reported E_0 and $E_{0,j}$ values also include the effects of increasing and decreasing the time assumed available for dissociation (10^{-4} s) by a factor of 2 and the sensitivity of our analysis to the values for the transitional modes (ascertained by multiplying and dividing the rota-

tional constants for these 1-D rotors by a factor of 2).

Equations (2) and (4) explicitly include the internal energy of the ion, E_i. All energy available is treated statistically, which should be a reasonable assumption because the internal (rotational and vibrational) energy of the reactants is redistributed throughout the ion upon impact with the collision gas. The threshold for dissociation is by definition the minimum energy required to lead to dissociation and thus corresponds to formation of products with no internal excitation. The assumption that products formed at threshold have an internal temperature of 0 K has been tested for several systems.[1,11,14–16] It has been shown that treating all energy of the ion (vibrational, rotational, and translational) as capable of coupling into the dissociation coordinate leads to reasonable thermochemistry. The threshold energies for dissociation reactions determined by analysis with Eqs. (2) and (4) are converted to 0 K bond energies by assuming that E_0 and $E_{0,j}$ represent the energy difference between reactants and products at 0 K.[39] This requires that there are no activation barriers in excess of the endothermicity of dissociation. This is generally true for ion-molecule reactions[35] and should be valid for the simple heterolytic bond fission reactions examined here.[40]

RESULTS

Figure 2 shows experimental cross sections for the interaction of Xe with several $(R_1OH)Li^+(R_2OH)$ complexes, where R_1OH, R_2OH=water, methanol, ethanol, 1-propanol, 2-propanol, or 1-butanol. A complete set of figures for all ten systems examined can be obtained from Ref. 32. The most favorable processes for all complexes are the loss of one of the intact ligands in the collision-induced dissociation (CID) reactions

$$(R_1OH)Li^+(R_2OH)+Xe \rightarrow Li^+(R_1OH)+R_2OH+Xe \rightarrow R_1OH+Li^+(R_2OH)+Xe. \quad (6)$$

These two processes are clearly in competition with one another as their shapes are distinctly different even in cases where the apparent thresholds are fairly close. Another indication of this is the smooth increase in the total cross section as a function of energy.

A number of minor products are also observed in these studies. The most dominant of these is sequential dissociation of both ligands to form atomic Li^+ ions. This generally has a cross section about one order of magnitude smaller than the primary products of reactions (6) at the highest energies studied. Another order of magnitude smaller are cross sections for products such as Li^+Xe, formed by ligand exchange processes. In some but not all cases, other ions with masses that could correspond to hydrocarbon cations, such as $C_3H_7^+$ and $C_4H_9^+$, or $C_2H_3O^+$ and $C_3H_5O^+$, were also observed with very small cross sections (less that 0.1 Å^2). It is possible that these latter species are formed by dissociation of minor components of the reactant ion beam that are hydrocarbon cations formed in the plasma of the flow tube source. Little systematic information can be gleaned from these products and they will not be discussed further.

Threshold analysis excluding competition

The model represented by Eq. (2) in which competition between channels is not included was used to analyze the thresholds for reactions (6) in ten $(R_1OH)Li^+(R_2OH)$ systems. The results of these analyses are provided in Table III. The experimental cross sections for reaction (6) in all ten systems are accurately reproduced using a loose phase space limit (PSL) TS model.[7] Good reproduction is obtained over energy ranges exceeding 2 eV and cross section magnitudes of at least a factor of 100. Table III includes three values of E_0: one that does not include the RRKM lifetime analysis and two where the lifetime analysis is included (a loose PSL and a tight TS model) as described above. The values obtained with no RRKM analysis should be very conservative upper limits to the true thermodynamic thresholds, while those obtained with a tight TS provide very conservative lower limits. The best values are expected to arise from the loose TS model, an assumption that has been tested in several systems previously.[1,3,7,37,38,41]

Comparison of the three E_0 values in Table III shows that the kinetic shifts (the difference in the thresholds obtained with and without consideration of the lifetime effect) vary with the size and geometry of the complexes. Dissociation of $(H_2O)Li^+(MeOH)$ shows a kinetic shift of less than 0.1 eV for a loose PSL TS and 0.1–0.2 eV when a tight TS is used. As the size of the alcohol increases, the kinetic shift gradually increases reaching a maximum for $(EtOH)Li^+(1\text{-}BuOH)$, which exhibits a kinetic shift of approximately 0.4 eV when determined with a loose PSL TS and over 0.6 eV when determined with a tight TS. This effect is largely due to the size of the systems. The $(H_2O)Li^+(MeOH)$ system has only 4 heavy atoms and 24 vibrational modes while the $(EtOH)Li^+(1\text{-}BuOH)$ system has 8 heavy atoms and 69 vibrational modes. As expected, the kinetic shifts are always larger for processes having higher energy thresholds.

The complexity of the system is also reflected by the entropies of activation, $\Delta S^\dagger$, a measure of the tightness or looseness of the TS. Listed in Table III at 1000 K, the $\Delta S^\dagger$ (PSL) values can be seen to increase from the smallest to the largest systems. These entropies of activation can be favorably compared to $\Delta S^\dagger_{1000}$ values in the range of 29–46 J/K mol collected by Lifshitz for several simple bond cleavage dissociations of ions.[42] Considering that the TS is expected to lie at the centrifugal barrier for association of $(R_2OH)Li^+ + R_1OH$, the negative entropies of activation obtained for the tight TS clearly indicate that this model provides a very conservative overestimate of the kinetic shift.

Threshold analysis including competition

The model represented by Eq. (4) in which competition between channels is included was also used to analyze the thresholds for reactions (6) in ten $(R_1OH)Li^+(R_2OH)$ systems. As the rates of decomposition are intrinsic to the branching ratio, the analyses with Eq. (4) must include either loose (PSL) or tight TSs. An example of the types of fits obtained using a loose phase space limit (PSL) TS model[7] is shown in Fig. 3(a) for the $(EtOH)Li^+(1\text{-}PrOH)$ complex. The

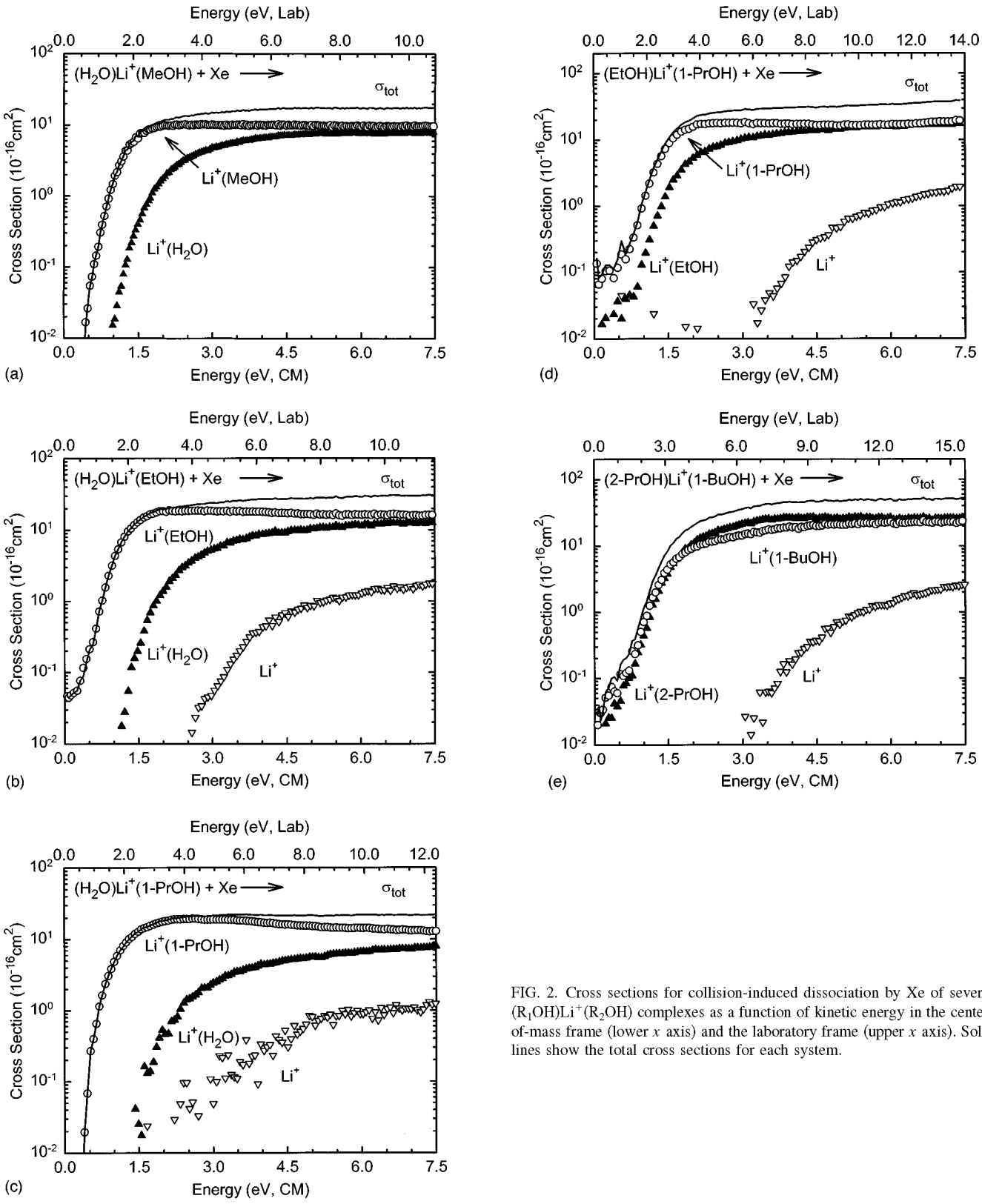

FIG. 2. Cross sections for collision-induced dissociation by Xe of several $(R_1OH)Li^+(R_2OH)$ complexes as a function of kinetic energy in the center-of-mass frame (lower x axis) and the laboratory frame (upper x axis). Solid lines show the total cross sections for each system.

only adjustable parameters in the analysis shown are $\sigma_{0,j}$, n, and $E_{0,j}$. In the fit shown, $\sigma_{0,1}$ and $\sigma_{0,2}$ were constrained to equal one another, such that the energy dependence of the branching between the two channels is handled exclusively by the statistical rate constants which have no additional adjustable parameters. This approach to analyzing the data worked well in four systems: $(MeOH)Li^+(EtOH)$, $(EtOH)Li^+(1\text{-}PrOH)$, $(EtOH)Li^+(2\text{-}PrOH)$, and $(2\text{-}PrOH)Li^+(1\text{-}BuOH)$. Good reproduction was obtained over energy ranges exceeding 2 eV and cross section mag-

TABLE III. Threshold dissociation energies at 0 K and entropies of activation at 1000 K of $(R_1OH)Li^+(R_2OH)$ obtained when competition is ignored and data sets are independently analyzed.[a]

Reactant complex	Ionic product	σ_0[b]	n[b]	E_0[c]	E_0(PSL)[c]	$\Delta S^{\ddagger}$(PSL)[d]	E_0(tight)[c]	$\Delta S^{\ddagger}$(tight)[d]
$(H_2O)Li^+(CH_3OH)$	$Li^+(H_2O)$	8 (1)	1.3 (0.1)	1.66 (0.05)	1.58 (0.05)	13 (9)	1.46 (0.05)	−3 (9)
	$Li^+(CH_3OH)$	19 (2)	1.2 (0.1)	1.21 (0.06)	1.11 (0.06)	11 (9)	1.05 (0.05)	−10 (9)
$(H_2O)Li^+(C_2H_5OH)$	$Li^+(H_2O)$	8 (1)	1.5 (0.1)	1.74 (0.08)	1.64 (0.08)	35 (9)	1.44 (0.07)	5 (9)
	$Li^+(C_2H_5OH)$	33 (1)	1.2 (0.1)	1.14 (0.08)	1.05 (0.07)	19 (9)	0.96 (0.06)	−10 (9)
$(H_2O)Li^+(1\text{-}C_3H_7OH)$	$Li^+(H_2O)$	7 (1)	1.3 (0.1)	2.09 (0.07)	1.82 (0.11)	35 (9)	1.54 (0.10)	3 (9)
	$Li^+(1\text{-}C_3H_7OH)$	32 (3)	1.0 (0.1)	1.22 (0.14)	1.10 (0.10)	8 (9)	1.01 (0.09)	−11 (9)
$(CH_3OH)Li^+(C_2H_5OH)$	$Li^+(CH_3OH)$	13 (1)	1.4 (0.1)	1.63 (0.06)	1.49 (0.06)	31 (10)	1.28 (0.06)	−2 (10)
	$Li^+(C_2H_5OH)$	30 (3)	1.0 (0.1)	1.37 (0.06)	1.25 (0.06)	19 (9)	1.10 (0.05)	−4 (9)
$(CH_3OH)Li^+(1\text{-}C_3H_7OH)$	$Li^+(CH_3OH)$	8 (1)	1.4 (0.1)	1.85 (0.09)	1.59 (0.10)	36 (9)	1.18 (0.09)	4 (9)
	$Li^+(1\text{-}C_3H_7OH)$	44 (8)	1.3 (0.1)	1.28 (0.09)	1.14 (0.07)	14 (9)	1.07 (0.06)	−5 (9)
$(C_2H_5OH)Li^+(1\text{-}C_3H_7OH)$	$Li^+(C_2H_5OH)$	17 (1)	1.1 (0.1)	1.71 (0.07)	1.44 (0.08)	41 (9)	1.16 (0.07)	6 (9)
	$Li^+(1\text{-}C_3H_7OH)$	38 (1)	0.9 (0.1)	1.57 (0.08)	1.33 (0.07)	30 (9)	1.11 (0.07)	0 (9)
$(C_2H_5OH)Li^+(2\text{-}C_3H_7OH)$	$Li^+(C_2H_5OH)$	11 (1)	1.5 (0.1)	1.75 (0.09)	1.47 (0.09)	42 (9)	1.18 (0.09)	1 (9)
	$Li^+(2\text{-}C_3H_7OH)$	42 (1)	0.9 (0.1)	1.64 (0.09)	1.39 (0.08)	37 (9)	1.12 (0.08)	−2 (9)
$(C_2H_5OH)Li^+(1\text{-}C_4H_9OH)$	$Li^+(C_2H_5OH)$	19 (5)	1.7 (0.6)	1.84 (0.24)	1.44 (0.15)	30 (13)	1.21 (0.13)	5 (13)
	$Li^+(1\text{-}C_4H_9OH)$	71 (5)	0.6 (0.5)	1.87 (0.15)	1.44 (0.12)	24 (9)	1.20 (0.12)	−2 (9)
$(1\text{-}C_3H_7OH)Li^+(1\text{-}C_4H_9OH)$	$Li^+(1\text{-}C_3H_7OH)$	24 (5)	1.5 (0.3)	1.62 (0.19)	1.30 (0.12)	41 (13)	1.04 (0.11)	6 (13)
	$Li^+(1\text{-}C_4H_9OH)$	37 (10)	1.3 (0.4)	1.51 (0.20)	1.26 (0.13)	48 (13)	0.99 (0.11)	4 (13)
$(2\text{-}C_3H_7OH)Li^+(1\text{-}C_4H_9OH)$	$Li^+(2\text{-}C_3H_7OH)$	37 (5)	1.3 (0.2)	1.65 (0.09)	1.28 (0.08)	28 (11)	1.04 (0.08)	2 (11)
	$Li^+(1\text{-}C_4H_9OH)$	25 (5)	1.3 (0.1)	1.54 (0.08)	1.21 (0.07)	31 (9)	0.98 (0.07)	0 (9)

[a]Uncertainties are listed in parentheses.
[b]Average values for loose PSL transition state.
[c]Units of eV.
[d]Units of J/K mol.

nitudes of at least a factor of 100. Considering that there are no adjustable parameters for controlling the energy dependence of the branching ratios of these analyses, the accurate reproduction of both decomposition channels is remarkable. This provides evidence that the assumption of loose (PSL) transition states is an appropriate means of interpreting CID data.

For six of the complexes studied, the data could not be reproduced accurately using Eq. (4) unless $\sigma_{0,1}$ and $\sigma_{0,2}$ were no longer constrained to equal one another. When this constraint was applied, the relative magnitudes of the channels were not accurately predicted by the k_j/k_{tot} term in Eq. (4), although severe discrepancies were observed only for $(MeOH)Li^+(H_2O)$ and $(EtOH)Li^+(H_2O)$. An example of this type of fit is shown in Fig. 3(b) for the $(EtOH)Li^+(H_2O)$ complex. It can be seen that the reproduction of the higher energy $Li^+(H_2O)$ channel is especially poor. The threshold for this channel is clearly too low while that for $Li^+(EtOH)$ is slightly higher than should be optimum for reproduction of the data. The situation is much worse for the $(MeOH)Li^+(H_2O)$ system. Several possible explanations for this disparity were explored, such as a failure to properly include symmetry numbers. No satisfactory explanation was achieved so the ability to allow the relative magnitudes of the cross section channels to vary empirically was introduced through the channel dependent $\sigma_{0,j}$ values. This flexibility introduces additional adjustable parameters into Eq. (4) that equal the number of channels minus one; e.g., for the two channel systems discussed here, this introduces a single adjustable parameter that is energy independent. When this adjustment to the fitting procedure is introduced, the data for the remaining six systems can be reproduced with excellent fidelity. Optimum fitting parameters for all ten systems are provided in Table IV. Figure 4 shows such fits for five of the systems examined including the example of the $(H_2O)Li^+(MeOH)$ system, the case showing the largest deviation from equal values of $\sigma_{0,1}$ and $\sigma_{0,2}$. Also compare the reproduction of the $(EtOH)Li^+(H_2O)$ system in Fig. 4(b) with that in Fig. 3(b). A complete set of figures showing this type of analysis is included in Ref. 32. The relative thresholds obtained from these analyses are in good agreement with those measured directly in previous experiments, as discussed further below. It is important to note that the statistical theory still successfully predicts the energy dependence of the branching ratio, but the relative magnitudes are now allowed to vary more freely.

The nature of the relative scaling parameter, $\sigma_{0,1}/\sigma_{0,2}$ where channel 2 has the lower threshold energy, can be explored by examination of several systems. We note that the value of $\sigma_{0,1}/\sigma_{0,2}$ needed to reproduce the $(ROH)Li^+(H_2O)$ systems gradually decreases as ROH increases in size, from 4.7 for MeOH to 2.1 for EtOH to 0.8 for 1-PrOH. The size of the scaling parameter is inversely related to the difference in threshold energies, which is counterintuitive if it were related to the thermodynamics of the system. We also considered whether this might be an artifact associated with mass discrimination in the quadrupole mass filter or inefficiencies in the collection of product ions. However, we would expect mass discrimination to be most severe as the difference in mass between H_2O and ROH increases, whereas the opposite effect is observed. If there were collection efficiency problems, we would expect that heavier mass products, which are located closer to the center of mass velocity, would be preferentially detected, while we observe an apparent enhancement in the $Li^+(H_2O)$ cross sections relative to the $Li^+(MeOH)$ and $Li^+(EtOH)$ cross sections. We also note that

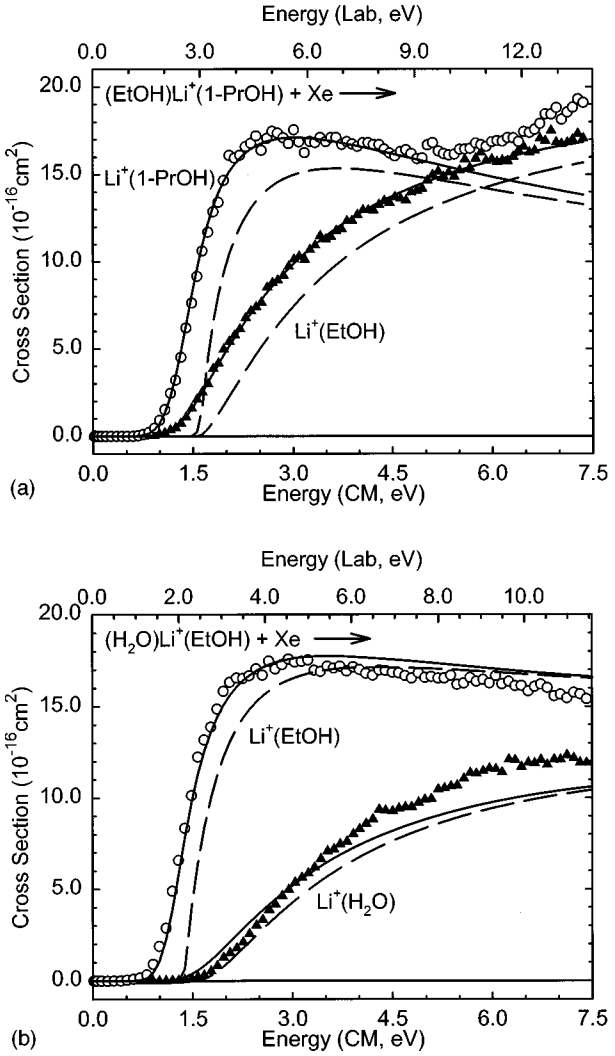

FIG. 3. Cross sections for collision-induced dissociation by Xe of (EtOH)Li^+(1−PrOH) (a) and (H_2O)Li^+(EtOH) (b) complexes in the threshold region as a function of kinetic energy in the center-of-mass frame (lower x axis) and the laboratory frame (upper x axis). Solid lines show the best fits to the data for both channels using the model of Eq. (4) with $\sigma_{0,1}=\sigma_{0,2}$ convoluted over the neutral and ion kinetic and internal energy distributions. Dashed lines show the model cross sections in the absence of experimental kinetic energy broadening for reactants with an internal energy of 0 K.

all systems that could be reproduced with $\sigma_{0,1}=\sigma_{0,2}$ have ligands that differ by only a single methylene group. It seems reasonable that pure statistical behavior would model competition between dissociation of similar ligands more accurately than dissimilar ligands. Small deviations from $\sigma_{0,1}=\sigma_{0,2}$ can plausibly be attributed to experimental limitations (such as mass discrimination and collection efficiency), but it seems clear that some other effect, not yet understood, is operative. Some possible effects that we are in the process of investigating include the inclusion of the ROH dipole moment in the evaluation of the variational transition state, the effect of treating the alcohol torsions as rotors rather than as vibrators, and more accurate determination of the rotational constants of the complexes.

The relative scaling parameters in the (ROH)Li^+(H_2O) systems vary in such a fashion that the larger systems behave more statistically than smaller systems, as might be expected for increased degrees of freedom available for energy randomization. This is possibly an indication that the dynamics of the dissociation process can be important for sufficiently small ligands. One conceivable mechanism might relate to an enhanced probability of exciting the larger ROH ligand versus the smaller H_2O ligand during the initial collision with Xe, followed by a failure to randomize energy completely before dissociation occurs in these relatively smaller systems. However, one of the larger systems examined, (1-PrOH)Li^+(1-BuOH), also shows a relatively large $\sigma_{0,1}/\sigma_{0,2}$ value, 1.7, suggesting that this behavior does not have a dynamic origin.

We also attempted to reproduce the data using Eq. (4) with a tight transition state as described above. None of these fits could accurately reproduce the data regardless of the energy range chosen for analysis. Further, such attempts at fitting the data yield relative thresholds that are much too small compared with literature thermochemistry. These observations are a clear demonstration that the assumption of tight transition states is inappropriate for such CID systems and that the absolute threshold values obtained from tight transition states are much too low. Considering that both the loose (PSL) and tight models adequately reproduce single channel CID cross sections well,[3] the failure of the tight TS model in these competitive multichannel CID processes underscores the success of the PSL model in the present work.

DISCUSSION

Relative lithium ion binding affinities

The clearest way of examining the influence of competition on the threshold analyses is to examine the relative thresholds for reactions (6), E_{rel}. It should be realized that although the thresholds for these two processes are direct measurements of the binding energy of the second ligand, the difference between these thresholds, $E_{rel}=D(R_1OHLi^+-R_2OH)-D(R_2OHLi^+-R_1OH)$, also equals the difference between the binding energies of the first ligand, $E_{rel}=D(Li^+-R_2OH)-D(Li^+-R_1OH)$. This follows simply from the observation that the sum of the two bonds in (R_1OH)Li^+(R_2OH) does not depend on which ligand is removed first. The differences between the thresholds measured for the two channels are listed in Table V. Values obtained by analyzing the two cross sections independently with Eq. (2) and including competition with Eq. (4) are provided. The latter values have much smaller uncertainties because the difference between the two channels varied much less from data set to data set and with changes in frequencies than the absolute values of the thresholds. It can be seen that the values measured including competition are smaller or equivalent to the difference in the independently measured values. The only exception is the (C_2H_5OH)Li^+(1-C_4H_9OH) system which is clearly anomalous. It is important to note that the differences in the independently measured values are much more sensitive to the noise in the data, while the requirement of fitting multiple dissociation channels constrains the competitive fits much more closely and makes these analyses much less sensitive to such anomalous data.

To ascertain which of these methods of determining the

TABLE IV. Threshold dissociation energies at 0 K and entropies of activation at 1000 K of $(R_1OH)Li^+(R_2OH)$ obtained when competition is included.[a]

Reactant complex	ionic product	σ_0[b]	n[b]	E_0(PSL)[c]	$\Delta S^{\ddagger}$(PSL)[d]	ΔE_0(PSL)[c]
$(H_2O)Li^+(CH_3OH)$	$Li^+(H_2O)$	90 (7)	0.9 (0.1)	1.39 (0.05)	13 (10)	0.239 (0.012)
	$Li^+(CH_3OH)$	19 (2)		1.15 (0.05)	11 (9)	
$(H_2O)Li^+(C_2H_5OH)$	$Li^+(H_2O)$	74 (2)	0.8 (0.1)	1.46 (0.06)	33 (10)	0.294 (0.011)
	$Li^+(C_2H_5OH)$	36 (1)		1.16 (0.05)	18 (9)	
$(H_2O)Li^+(1\text{-}C_3H_7OH)$	$Li^+(H_2O)$	28 (1)	0.9 (0.1)	1.46 (0.07)	34 (9)	0.321 (0.012)
	$Li^+(1\text{-}C_3H_7OH)$	36 (1)		1.14 (0.06)	8 (9)	
$(CH_3OH)Li^+(C_2H_5OH)$	$Li^+(CH_3OH)$	40 (4)	1.2 (0.1)	1.36 (0.05)	31 (10)	0.127(0.004)
	$Li^+(C_2H_5OH)$	35 (4)		1.23 (0.05)	19 (10)	
$(CH_3OH)Li^+(1\text{-}C_3H_7OH)$	$Li^+(CH_3OH)$	15 (1)	1.4 (0.1)	1.35 (0.06)	38 (9)	0.170 (0.010)
	$Li^+(1\text{-}C_3H_7OH)$	31 (1)		1.18 (0.06)	14 (9)	
$(C_2H_5OH)Li^+(1\text{-}C_3H_7OH)$	$Li^+(C_2H_5OH)$	50 (2)	0.8 (0.1)	1.46 (0.07)	41 (9)	0.085 (0.002)
	$Li^+(1\text{-}C_3H_7OH)$	54 (2)		1.37 (0.07)	30 (9)	
$(C_2H_5OH)Li^+(2\text{-}C_3H_7OH)$	$Li^+(C_2H_5OH)$	60 (4)	1.1 (0.1)	1.45 (0.07)	43 (9)	0.098 (0.003)
	$Li^+(2\text{-}C_3H_7OH)$	47 (2)		1.36 (0.07)	37 (9)	
$(C_2H_5OH)Li^+(1\text{-}C_4H_9OH)$	$Li^+(C_2H_5OH)$	107 (24)	0.7 (0.1)	1.56 (0.09)	39 (9)	0.153 (0.023)
	$Li^+(1\text{-}C_4H_9OH)$	83 (5)		1.40 (0.10)	24 (9)	
$(1\text{-}C_3H_7OH)Li^+(1\text{-}C_4H_9OH)$	$Li^+(1\text{-}C_3H_7OH)$	86 (22)	1.3 (0.3)	1.35 (0.12)	52 (9)	0.056 (0.018)
	$Li^+(1\text{-}C_4H_9OH)$	52 (15)		1.29 (0.12)	48 (9)	
$(2\text{-}C_3H_7OH)Li^+(1\text{-}C_4H_9OH)$	$Li^+(2\text{-}C_3H_7OH)$	60 (8)	1.3 (0.1)	1.29 (0.07)	40 (9)	0.030 (0.024)
	$Li^+(1\text{-}C_4H_9OH)$	70 (36)		1.26 (0.07)	30 (9)	

[a]Uncertainties are listed in parentheses.
[b]Average values for loose PSL transition state.
[c]Units of eV.
[d]Units of J/K mol.

relative thresholds is more correct, Table V includes a comparison with differences calculated from our previous study of the CID of monoligated lithium ions.[3] As a further check, Table V includes differences measured by Taft *et al.* using equilibrium methods in an ICR mass spectrometer.[6] The ICR values have been adjusted from 373 K values to 0 K values using information in Ref. 3. These two sets of literature values are mutually consistent except for the three values involving 1-butanol, where the direct CID values lie about 0.10 eV lower than the ICR values. This is easily seen in Fig. 5 which shows the three sets of CID numbers vs the ICR values. The direct CID values taken from our previous work fall very close to the line having a slope of unity, except for the three values associated with 1-butanol which are parallel to this line. This discrepancy, discussed previously,[3] is further elucidated by the present work as detailed below.

Examination of the four sets of values listed in Table V and of Fig. 5 makes it clear that the relative thresholds determined by including explicit consideration of the competition agree better with the literature values in all cases, while the independently analyzed thresholds give differences that are too large in most cases and too small for the $(ROH)Li^+(1\text{-BuOH})$ systems, most obvious for ROH=EtOH. A linear regression analysis (constrained to include the origin) finds that the independently determined threshold differences exceed the ICR results by a factor of about 2. In contrast, the competitive E_{rel} values have an average deviation from the literature ICR values of 0.003 $\pm$0.028 eV.

In those cases where the complexes contain 1-butanol as one of the ligands, the analysis including competition provides relative thresholds in good agreement with the ICR results, but shifted from our direct CID measurements by an average of 0.08$\pm$0.01 eV. (The direct CID measurements are shifted from the ICR results by an average of 0.10 $\pm$0.01 eV.) In our previous work,[3] excellent agreement between the lithium ion–alcohol bond energies measured by direct CID and those determined from ICR results (after correctly adjusting for temperature) was obtained for all but two alcohols: 1-butanol and *i*-butanol (2-methyl-1-propanol). The present measurements make it clear that the Li^+–1-butanol bond energy obtained by direct CID is systematically low. This could occur if the kinetic shift in this case was too large, which in turn could result from a transition state that was too tight or a $Li^+(1\text{-}C_4H_9OH)$ complex that was too loose. Further, the cause of this excessive kinetic shift would have to be something unlikely to affect the other alcohols (certainly the smaller ones) as drastically. 1-butanol is unique in that it has the longest carbon chain of any alcohol considered in our previous work.[3] One possible way that the transition state could be looser than the already loose PSL TS is to treat the torsional modes of butanol as free rotors rather than as vibrators. It is also possible that the calculations on the $Li^+(1\text{-BuOH})$ complex underestimated the binding especially of the longer chain such that these same torsional motions are grossly hindered in the complex. Further studies of these possibilities and those associated with the influence of the dipole moment of the alcohols are being explored.

Competition

The previous section affirms that the methodology introduced here for including the effects of competition on CID thresholds is a valuable one that is capable of yielding accurate thermochemistry. In addition, the unconvoluted fits of

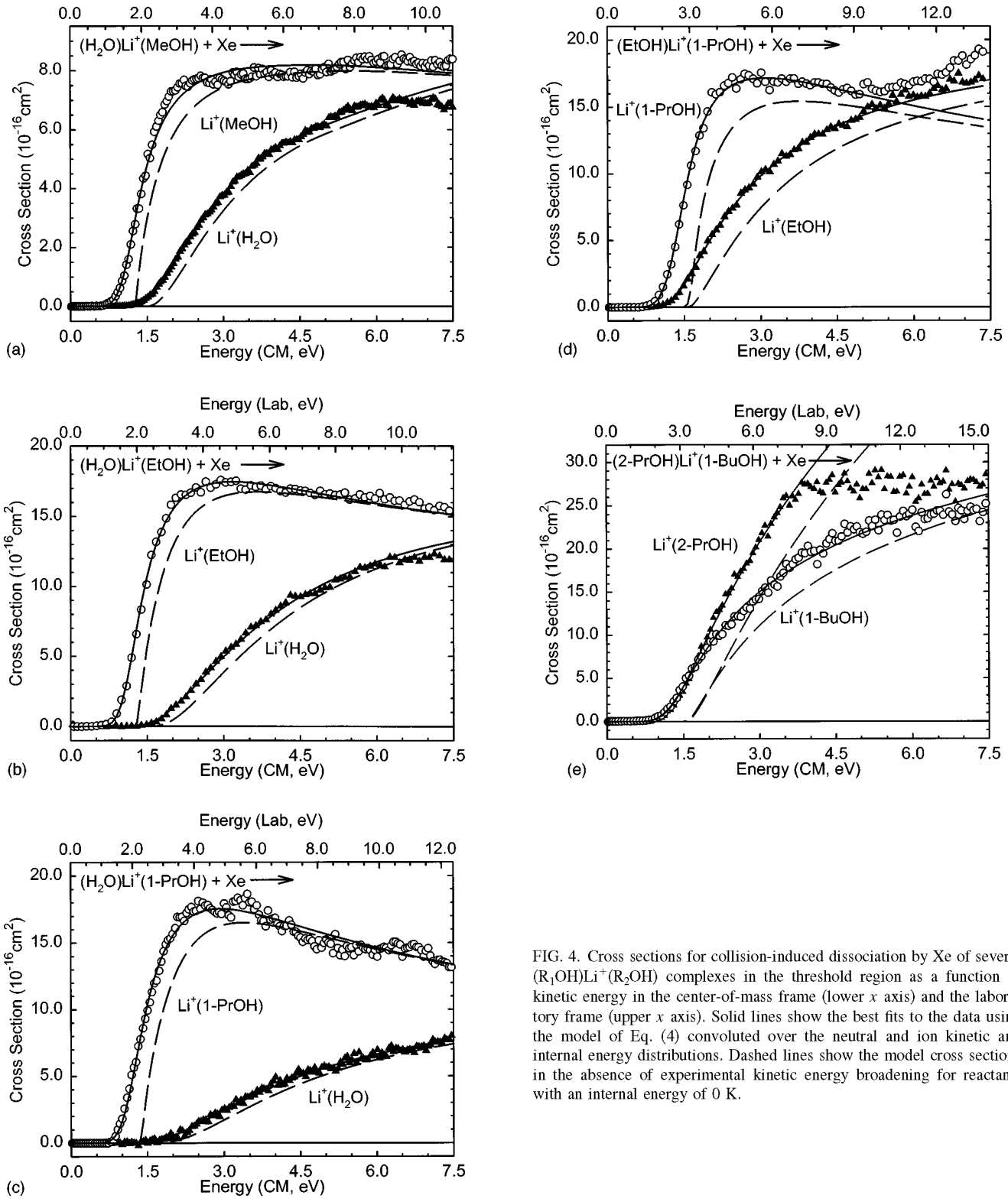

FIG. 4. Cross sections for collision-induced dissociation by Xe of several $(R_1OH)Li^+(R_2OH)$ complexes in the threshold region as a function of kinetic energy in the center-of-mass frame (lower x axis) and the laboratory frame (upper x axis). Solid lines show the best fits to the data using the model of Eq. (4) convoluted over the neutral and ion kinetic and internal energy distributions. Dashed lines show the model cross sections in the absence of experimental kinetic energy broadening for reactants with an internal energy of 0 K.

our data provide a detailed picture of just how severe the competition between channels can be. For example, in the $(EtOH)Li^+(1\text{-}PrOH)$ complex, the relative thresholds for loss of EtOH and 1-PrOH, differ by only 0.08 eV. This is obvious from the dashed lines in Fig. 4(d). The channel with the lower energy threshold rises very rapidly with energy while the higher energy process rises much more slowly. At higher kinetic energies, the second channel becomes sufficiently large that the cross section for the lower energy channel ceases to rise and either levels off or declines due to the competition. Because of the slow rise in the cross section for the higher energy channel, analysis of this cross section without explicit consideration of the competition provides thresholds that can be too high. The error in such an analysis is small for competitive channels with similar thresholds (different by less than about 0.1 eV), but increases as the

TABLE V. Direct versus competitive determination of relative Li^+ binding energies to ROH at 0 K (eV).

		$D_0(R_2OHLi^+-R_1OH)-D_0(R_1OHLi^+-R_2OH)$		$D_0(Li^+-R_1OH)-D_0(Li^+-R_2OH)$		
R_1OH	R_2OH	Independent[a]	Competitive[b]	Direct CID[c]	ICR equilibrium[d]	Best E_{rel}
CH_3OH	H_2O	0.47 (0.07)	0.239 (0.012)	0.226 (0.165)	0.205	0.204 (0.026)
C_2H_5OH	H_2O	0.60 (0.10)	0.294 (0.011)	0.314 (0.156)	0.287	0.300 (0.030)
1-C_3H_7OH	H_2O	0.72 (0.15)	0.321 (0.012)	0.385 (0.166)	0.357	0.370 (0.026)
C_2H_5OH	CH_3OH	0.23 (0.08)	0.127 (0.004)	0.088 (0.111)	0.082	0.096 (0.021)
1-C_3H_7OH	CH_3OH	0.17 (0.16)	0.170 (0.010)	0.159 (0.125)	0.152	0.167 (0.018)
1-C_3H_7OH	C_2H_5OH	0.11 (0.10)	0.085 (0.002)	0.071 (0.112)	0.070	0.071 (0.016)
2-C_3H_7OH	C_2H_5OH	0.08 (0.13)	0.098 (0.003)	0.097 (0.103)	0.090	0.093 (0.016)
1-C_4H_9OH	C_2H_5OH	0.00 (0.19)	0.153 (0.023)	0.054 (0.108)[e] [0.144][f]	0.155	0.144 (0.021)
1-C_4H_9OH	1-C_3H_7OH	0.04 (0.18)	0.056 (0.018)	−0.017 (0.123)[e] [0.073][f]	0.084	0.073 (0.017)
1-C_4H_9OH	2-C_3H_7OH	0.06 (0.11)	0.030 (0.024)	−0.043 (0.115)[e] [0.047][f]	0.064	0.051 (0.016)

[a]Difference in E_0(PSL) values between channels from Table III.
[b]Difference in E_0(PSL) values between channels from Table IV.
[c]Difference in thresholds from Refs. 1 and 3.
[d]Difference in enthalpies of values from Ref. 6 after correction to 0 K as outlined in Ref. 3.
[e]Values excluded in determining best E_{rel} values.
[f]Values increased by 0.09 eV. See the text.

difference in relative thresholds increases (Fig. 5). One can also envision systems in which the process having the higher lying threshold is entropically favored by a big enough factor to overcome even a large enthalpic difference (e.g., competition between a low energy, tight transition state and a high energy, loose transition state), in which case, the competitive shift may again decrease. Studies of such systems are presently under investigation in our laboratory.

The methodology introduced here also properly handles the interesting case of (2-PrOH)Li^+(1-BuOH) in which the higher energy channel, formation of Li^+(2-PrOH) is the favored product at higher collision energies, i.e., the two cross sections cross one another. In this regard, we note that the entropically favored reaction channel is the higher energy channel for all systems (see $\Delta S^\dagger$ in Table IV). Generally, the threshold difference between channels is sufficiently large that the energetically favored channel is dominant over the energy range examined. The case of (2-PrOH)Li^+(1-BuOH) has the smallest E_{rel} value of all systems examined (Table V) leading to the observed crossing in the magnitudes of the cross sections for the two channels. This behavior has implications for the widely applied kinetic method,[43] which generally makes the assumption that entropic factors for similar ligands are equal, and hence that the relative intensities of products formed by competitive dissociation accurately reflect the relative energetics. In the (2-PrOH)Li^+(1-BuOH) case, such an assumption would lead to the incorrect conclusion that $D(Li^+-2\text{-PrOH}) > D(Li^+-1\text{-BuOH})$.

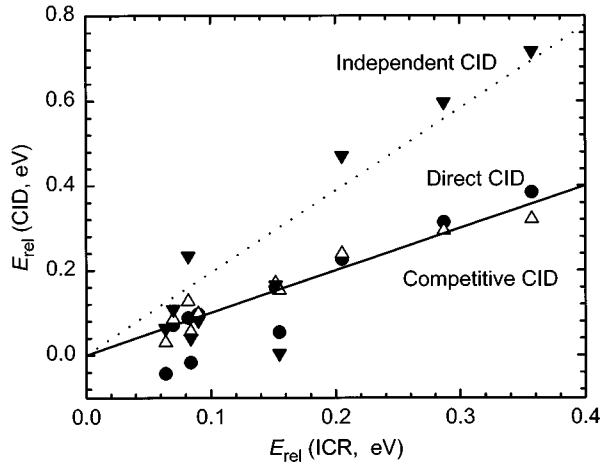

FIG. 5. Relative threshold differences between competitive dissociation channels measured by collision induced dissociation vs those measured in ICR equilibrium studies (Ref. 6). Closed circles show values determined previously by direct CID of Li^+(ROH) complexes (Refs. 1 and 3), closed triangles show those determined by fitting the two reaction channels independently using Eq. (2), and open triangles show those determined by analysis including competition using Eq. (4). All values taken from Table V.

Lithium ion binding affinities for the first ligand: Integration of relative and absolute values

We now need to integrate the various ladders of relative lithium ion binding affinities contained in Table V in order to provide best values for the primary ligand affinities. Although there are several ways in which this can be accomplished, the final E_{rel} values must be self-consistent. We chose to use the Li^+-CH_3OH, $Li^+-C_2H_5OH$, Li^+-1-C_3H_7OH, and Li^+-2-C_3H_7OH bond energies measured by direct CID[3] as our primary standards. These absolute bond energies are combined with the three (competitive CID, direct CID, and ICR) relative threshold values to yield a series of absolute values for the six Li^+–ROH bond energies. Direct CID, values for E_{rel} involving 1-BuOH were not used in this procedure. The average of all the resulting values yields the final absolute values listed in Table VI and differences between these values given as best E_{rel} values in Table V. The absolute values obtained are in excellent agreement with all previously determined absolute values except for 1-butanol where the present value is 0.09 eV higher than that determined by direct CID.[3] This is consistent with our dis-

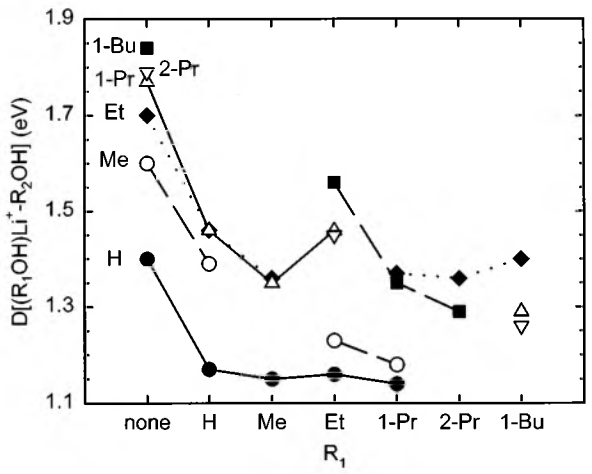

FIG. 6. Absolute bond dissociation energies (in eV) for $(R_1OH)Li^+-R_2OH$ as a function of the R_1OH ligand, where R_2=H (closed circles), CH_3 (open circles), C_2H_5 (closed diamonds), 1-C_3H_7 (open triangles), 2-C_3H_7 (inverted triangles), and 1-C_4H_9 (closed squares). Values taken from Table VI.

cussion above concerning the reliability of this particular CID value. The best E_{rel} values are also consistent with simple averages of the three (two for systems involving 1-BuOH) E_{rel} values in Table V.

Lithium ion binding affinities for the second ligand

As noted above, the thresholds measured in the present system provide 0 K bond energies for the second alcohol ligand bound to Li^+. Our experimental results (determined with threshold analyses corrected for lifetime effects assuming a loose PSL TS including consideration of competition) at 0 K are listed in Table VI and shown in Fig. 6. Table VII lists these values converted to 298 K for ease in comparison with other experiments. These tables also compare these values with the binding energies of the first ligand.[1,3] In all cases, the second ligand binding energies are weaker than the first, consistent with simple ideas of electrostatic bonding. The decline is reasonably uniform, varying from about 0.2 eV for $(ROH)Li^+-OH_2$ to 0.3 eV for $(ROH)Li^+$–1-C_3H_7OH. For most ligands, the second ligand binding energy is fairly uniform, e.g., all $(ROH)Li^+-OH_2$ are about 1.2 eV and all $(ROH)Li^+-C_2H_5OH$ are about 1.4 eV. Some variations occur such that smaller ligands induce a smaller decrease from the first bond energy than larger ligands, e.g., $(H_2O)Li^+-CH_3OH$ is greater than $(ROH)Li^+-CH_3OH$ when ROH=C_2H_5OH or 1-C_3H_7OH. Similarly, (1-C_4H_9OH)Li^+– ROH is weaker than other $(R_1OH)Li^+$–ROH bond energies for ROH=1-C_3H_7OH and 2-C_3H_7OH, but not for C_2H_5OH. In the former case, this probably reflects the observation that the Li^+-H_2O bond energy is the weakest of all Li^+–ROH species, indicating that the extent of electron donation to the metal ion by water is the least. The latter case involving the 1-butanol system is conceivably explained by more severe steric interactions between larger ligands. Referring to Fig. 1, it can be seen that these ligands tend to wrap around the lithium ion such that the larger ligands may interfere with one another. In the case of 1-BuOH, this effect is indicated by the observation that the optimum structure for Li^+(1-BuOH) has all four carbons wrapped around the lithium ion,[3] while the optimum structures for $(ROH)Li^+$(1-BuOH) have only a three carbon chain wrapped around the lithium (Fig. 1). (Geometry optimization of structures started with the 4-carbons wrapped around the Li^+ always relaxed to the geometries shown.) It seems clear that steric interaction between the ligands forces the 1-butanol ligand into a structure that is more compact at the lithium center compared to the structure for the monoligated system.

Value for $D_0(Li^+-OH_2)$

The optimum value obtained here for the lithium ion affinity of water is 1.40±0.08 eV. This can be adjusted to a 298 K enthalpy of 139±8 kJ/mol. This value can be favorably compared to the estimate of Dzidic and Kebarle of 142±4 kJ/mol[2] and to the single experimental determination in the literature, our CID value of 137±14 kJ/mol.[1] This value also agrees with the best theoretical values in the literature which lie in a narrow range of 134–136 kJ/mol.[29,44]

CONCLUSIONS

The kinetic energy dependence of the collision-induced dissociation of $(R_1OH)Li^+(R_2OH)$, R_1OH, and R_2OH =water, methanol, ethanol, 1-propanol, 2-propanol, and 1-butanol, with Xe are examined in a guided ion beam mass spectrometer. The dominant dissociation processes in all

TABLE VI. Bond dissociation energies (in eV) of $(R_1OH)Li^+-R_2OH$ at 0 K.

	R_2OH					
R_1OH	H_2O	CH_3OH	C_2H_5OH	1-C_3H_7OH	2-C_3H_7OH	1-C_4H_9OH
None	1.40 (0.08)[a]	1.60 (0.08)[a]	1.70 (0.08)[a]	1.77 (0.08)[a]	1.79 (0.08)[a]	1.84 (0.08)[a]
H_2O	1.17 (0.10)[b]	1.39 (0.05)	1.46 (0.05)	1.46 (0.07)		
CH_3OH	1.15 (0.04)		1.36 (0.05)	1.35 (0.06)		
C_2H_5OH	1.16 (0.05)	1.23 (0.05)		1.46 (0.07)	1.45 (0.07)	1.56 (0.09)
1-C_3H_7OH	1.14 (0.06)	1.18 (0.06)	1.37 (0.07)			1.35 (0.12)
2-C_3H_7OH			1.36 (0.07)			1.29 (0.07)
1-C_4H_9OH			1.40 (0.10)	1.29 (0.12)	1.26 (0.07)	

[a]Best values determined as discussed in the text.
[b]Taken from Ref. 1.

TABLE VII. Bond dissociation energies (in kJ/mol) of $(R_1OH)Li^+-R_2OH$ at 298 K.

	R_2OH					
R_1OH	H_2O	CH_3OH	C_2H_5OH	1-C_3H_7OH	2-C_3H_7OH	1-C_4H_9OH
None	139 (8)[a]	156 (8)[a]	166 (8)[a]	173 (8)[a]	175 (8)[a]	180 (8)[a]
H_2O	114 (10)[b]	133 (5)	140 (5)	140 (7)		
CH_3OH	111 (4)		130 (5)	129 (6)		
C_2H_5OH	113 (5)	118 (5)		139 (7)	139 (7)	149 (9)
1-C_3H_7OH	110 (6)	112 (6)	130 (7)			129 (12)
2-C_3H_7OH			130 (7)			123 (7)
1-C_4H_9OH			133 (10)	123 (11)	119 (7)	

[a]Values taken from Table VI and temperature conversion according to Ref. 3.
[b]Taken from Ref. 1.

cases is formation of $Li^+(R_1OH)+R_2OH$ and $Li^+(R_2OH)+R_1OH$. Thresholds for these processes are determined after consideration of the effects of reactant internal energy, multiple collisions with Xe, and lifetime effects (using methodology described in detail elsewhere).[7] It is shown that the competition between the two dissociation channels must be explicitly considered in order to correctly interpret the CID thresholds. This is achieved by using statistical RRKM theory with a loose (phase space limit) transition state to predict the branching ratio between the two channels. No adjustable parameters are needed to accurately reproduce the branching ratios for some of the systems studied. For others, statistical theory does not predict the relative magnitudes of the competitive channels with high accuracy; however, by allowing the relative magnitudes of the two channels to be scaled, the kinetic energy dependence of the branching ratios is then well described by statistical theory. In either case, the relative thresholds of these competitive channels obtained by these analyses agree well with literature thermochemistry in all cases. This statistical approach provides a straightforward means of correcting for the competitive shift inherent in multichannel processes, although it entails a comprehensive evaluation of the molecular details of the processes being studied. First and second bond energies for the ROH molecules bound to lithium ions are obtained and a value for $D_0(Li^+-OH_2)=1.40\pm0.08$ eV is recommended.

ACKNOWLEDGMENTS

Funding for this work was provided by the National Science Foundation under Grant CHE-9530412 and partial funding by the Donors of the Petroleum Research Fund, administered by the American Chemical Society.

[1] M. T. Rodgers and P. B. Armentrout, J. Phys. Chem. A **101**, 1238 (1997).
[2] I. Dzidic and P. Kebarle, J. Phys. Chem. **74**, 1466 (1974).
[3] M. T. Rodgers and P. B. Armentrout, J. Phys. Chem. A **101**, 2614 (1997).
[4] R. H. Staley and J. L. Beauchamp, J. Am. Chem. Soc. **97**, 5920 (1975).
[5] R. L. Woodin and J. L. Beauchamp, J. Am. Chem. Soc. **100**, 501 (1978).
[6] R. W. Taft, F. Anvia, J.-F. Gal, S. Walsh, M. Capon, M. C. Holmes, K. Hosn, G. Oloumi, R. Vasanwala, and S. Yazdani, Pure Appl. Chem. **62**, 17 (1990).
[7] M. T. Rodgers, K. M. Ervin, and P. B. Armentrout, J. Chem. Phys. **106**, 4499 (1997).
[8] K. M. Ervin and P. B. Armentrout, J. Chem. Phys. **83**, 166 (1985).
[9] R. H. Schultz and P. B. Armentrout, Int. J. Mass Spectrom. Ion Processes **107**, 29 (1991).
[10] E. Teloy and D. Gerlich, Chem. Phys. **4**, 417 (1974); D. Gerlich, Diplomarbeit, University of Freiburg, Federal Republic of Germany, 1971; in *State-Selected and State-to-State Ion–Molecule Reaction Dynamics, Part I, Experiment*, edited by C.-Y. Ng and M. Baer, Adv. Chem. Phys. **82**, 1 (1992).
[11] N. F. Dalleska, K. Honma, and P. B. Armentrout, J. Am. Chem. Soc. **115**, 12125 (1993).
[12] N. Aristov and P. B. Armentrout, J. Phys. Chem. **90**, 5135 (1986).
[13] D. A. Hales and P. B. Armentrout, J. Cluster Sci. **1**, 127 (1990).
[14] N. F. Dalleska, K. Honma, L. S. Sunderlin, and P. B. Armentrout, J. Am. Chem. Soc. **116**, 3519 (1994).
[15] R. H. Schultz, K. C. Crellin, and P. B. Armentrout, J. Am. Chem. Soc. **113**, 8590 (1992).
[16] F. A. Khan, D. E. Clemmer, R. H. Schultz, and P. B. Armentrout, J. Phys. Chem. **97**, 7978 (1993).
[17] R. H. Schultz and P. B. Armentrout, J. Chem. Phys. **96**, 1046 (1992).
[18] E. R. Fisher, B. L. Kickel, and P. B. Armentrout, J. Phys. Chem. **97**, 10204 (1993).
[19] E. R. Fisher, B. L. Kickel, and P. B. Armentrout, J. Chem. Phys. **97**, 4859 (1992).
[20] T. S. Beyer and D. F. Swinehart, Commun. Assoc. Comput. Machines **16**, 379 (1973); S. E. Stein and B. S. Rabinovitch, J. Chem. Phys. **58**, 2438 (1973); Chem. Phys. Lett. **49**, 1883 (1977).
[21] R. G. Gilbert and S. C. Smith, *Theory of Unimolecular and Recombination Reactions* (Blackwell Scientific Publications, Oxford, 1990).
[22] D. G. Truhlar, B. C. Garrett, and S. J. Klippenstein, J. Phys. Chem. **100**, 12771 (1996).
[23] K. A. Holbrook, M. J. Pilling, and S. H. Robertson, *Unimolecular Reactions*, 2nd ed. (Wiley, New York, 1996).
[24] HYPERCHEM™ Computational Chemistry Software Package, Version 4.5, Hypercube Inc., 1996.
[25] J. J. P. Stewart, J. Comput. Chem. **10**, 209 (1989).
[26] J. J. P. Stewart, J. Comput. Chem. **10**, 221 (1989).
[27] E. Anders, R. Koch, and P. Freunscht, J. Comput. Chem. **14**, 1301 (1993).
[28] F. Anvia, S. Walsh, M. Capon, I. A. Koppel, R. W. Taft, J. L. G. de Paz, and J. Catalan, J. Am. Chem. Soc. **112**, 5095 (1990).
[29] D. Feller, E. D. Glendening, R. A. Kendall, and K. A. Peterson, J. Chem. Phys. **100**, 4981 (1994).
[30] D. M. Seeger, C. Korzeniewski, and W. Kowalchyk, J. Phys. Chem. **95**, 6871 (1991).
[31] G. Fogarasi and P. Pulay, in *Vibrational Spectra and Structure*, edited by J. R. Durig (Elsevier, New York, 1985), Vol. 14, p. 125.
[32] See AIP document No. PAPS JCPSA6-109-027829 for 25 pages of tables and figures. Order by PAPS number and journal reference from American Institute of Physics, Physics Auxiliary Publication Service, Carolyn Gehlbach, 500 Sunnyside Boulevard, Woodbury, New York 11797-2999. Fax: 516-576-2223, e-mail: paps@aip.org. The price is $1.50 for each microfiche (98 pages) or $5.00 for photocopies of up to 30 pages, and $0.15 for each additional page over 30 pages. Airmail additional. Make checks payable to the American Institute of Physics.
[33] E. V. Waage and B. S. Rabinovitch, Chem. Rev. **70**, 377 (1970).
[34] W. J. Chesnavich and M. T. Bowers, J. Phys. Chem. **83**, 900 (1979).
[35] P. B. Armentrout, in *Advances in Gas Phase Ion Chemistry*, edited by N. G. Adams and L. M. Babcock (JAI, Greenwich, 1992), Vol. 1, pp. 83–119.

[36] See, for example, L. S. Sunderlin and P. B. Armentrout, Int. J. Mass Spectrom. Ion Processes **94**, 149 (1989).
[37] M. B. More, E. D. Glendening, D. Ray, D. Feller, and P. B. Armentrout, J. Phys. Chem. **100**, 1605 (1996).
[38] D. Ray, D. Feller, M. B. More, E. D. Glendening, and P. B. Armentrout, J. Phys. Chem. **100**, 16116 (1996).
[39] See for example, Fig. 1 in Ref. 11.
[40] P. B. Armentrout and J. Simons, J. Am. Chem. Soc. **114**, 8627 (1992).
[41] F. Meyer, F. A. Khan, and P. B. Armentrout, J. Am. Chem. Soc. **117**, 9740 (1995).
[42] C. Lifshitz, Adv. Mass Spectrom. **11**, 113 (1989).
[43] S. A. McLuckey, D. Cameron, and R. G. Cooks, J. Am. Chem. Soc. **103**, 1313 (1981).
[44] J. E. Del Bene and I. Shavitt, Int. J. Quantum Chem. **24**, 365 (1990).